

Photo-induced currents in large area multiwalled CNT films/Al Structure

Jie Zhang (张 洁)^{1*}, Yulin Chen (陈俞霖)¹, Yong Zhu (朱 永)¹, and Fei Luo (骆 飞)²

¹The Key Laboratory for Optoelectronic Technology & System, Education Ministry of China, Chongqing University, Chongqing 400044, China

²FLT Inc, 405 Waltham St. #306, Lexington, MA 02421, USA

*Corresponding author: zhangjie@cqu.edu.cn

Received July 29, 2013; accepted October 13, 2013; posted online March 25, 2014

Photoresponse of large-area multi-walled carbon nanotube (MWCNT) films is explored under laser illumination. The experiment shows that the photo-induced current shows nearly linear response to the bias voltage. The photocurrent depends on the laser illumination spot position, with the maximum photocurrent occurring at the metal–film interface, while the minimum photocurrent is observed between two electrodes. We are attributing this photo-generated exciton due to Schottky junction between Al electrodes and the CNTs, and electron's concentration effect. The sample device shows photo responsibility of 521 mA/W at a bias voltage of 2V, which indicates that this device can be developed as a position-sensitive photodetector.

OCIS codes: 040.5150, 040.5350.

doi: 10.3788/COL201412.S10402.

Carbon nanotubes (CNTs) have unique physical and chemical properties. Numerous studies have focused on the optical properties of single-walled CNT (SWCNT) and multi-walled CNT (MWCNT)^[1–5]. Particularly, the interaction of CNTs with light brings opportunities for the development of novel nano optoelectronic devices.

The photoconductivity of isolated SWCNTs has been studied by Freitag *et al.*^[6]. Levisky *et al.*^[7] investigated the photoconductivity of thin CNT random networks. The photoresponse was observed in macrobundles of the MWCNTs^[8–10]. The photoelectric response of MWCNT films from UV to visible light was analyzed^[11]. Feng *et al.*^[12] have studied the photoluminescence and photoelectric response characteristics of TiO₂ nanoparticles decorated with MWCNTs in ultraviolet radiation. The laser-induced photocurrents of large-area vertically aligned MWCNTs have also been studied^[13].

In a photoresponse study of CNTs, the mechanism of contact between CNTs and metal electrodes is an important issue because it is generally believed that there is a Schottky barrier between semi-conducting CNTs and metal electrode junctions. Several experiments of individual and bundles of SWCNTs and MWCNTs have demonstrated that photocurrent generates when light illuminates the CNTs/metal junctions^[14–16]. It was reported that photocurrent occurs at MWCNT and metal junction in a macroscopically long bundle of ordered MWCNTs^[17], disordered MWCNTs mat^[18] and MWCNT–CuS hybrid nanostructures^[19]. If the sample is a macroscopic film, a new effect must be introduced by the interaction between the CNTs and CNTs and metal electrode conjunctions.

In this paper, experimental studies on photoresponse effect in disordered MWCNT films/Al electrode structures are presented. The MWCNT films are deposited by chemical method at SiO₂ substrate. The

photoconductivity measurements have been performed under laser illumination in different positions including the electrodes, with different bias voltage on electrodes.

MWCNT films were prepared on SiO₂ substrate coated by separated Al electrodes with thickness of 200 nm. Purified disordered CNT raw materials (approximately 0.5 g) were dispersed in 100 mL ethanol and mixed by low-speed magnetic stirring (approximately 5 m), then agitated by long ultrasonic agitating (approximately 60 m) to make sure uniform dispersion of CNT suspension. MWCNT suspensions were transferred to the substrate and heated.

Figure 1 shows a scanning electron microscopy (SEM) photo. The distance between two Al electrodes is 10 mm. Different amounts of disordered CNTs lead to different thickness and the resistance of the films.

Figure 2 shows the Raman spectra of the MWCNT film excited by a 532 nm laser. The intense bands at the vicinity of 1340 and 1569 cm⁻¹ are the D band

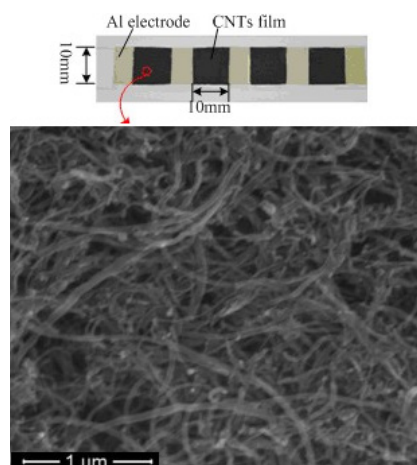


Fig. 1. Photo and SEM image of MWCNT film sample.

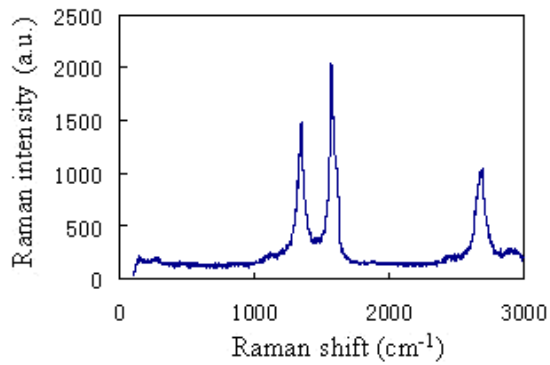


Fig. 2. Raman scattering spectra of the MWCNT film.

involved with the vibration mode and G band indicating the existence of disordered MWCNTs^[20,21].

The photoconductivity of the MWCNT films was carried out using the standard two-probe technique (Fig. 3), both illumination off and under illumination positioned at the MWCNT film samples, at room temperature, by a diode laser with a center wavelength of 532 nm, with power ranging from 5 to 24 mW as the illumination source. Data were collected by galvanometer (KEITHLEY 2002, current sensitivity of 10 pA).

Positions A and G are positive and negative electrodes, respectively; positions B and F are the spots of metal–MWCNT interface; D is the middle of the sample. The current was separately collected during *laser off* and *laser on*, and the net photocurrent I_p was the current with laser illumination subtracted by the dark current I_d without laser illumination.

To elucidate the role of the MWCNT–Al interface, the illumination position effect was investigated. In order to reduce the effect of Joule heating^[22] in large extent, there was no bias voltage. The net photocurrent as a function of the illuminating position repeated on different samples (the four samples were fabricated with the same materials and processes) exhibited similar results (Fig. 4). It can be observed that the photocurrent reaches the maximum when the interfaces are illuminated. The whole shape of the curve is nearly

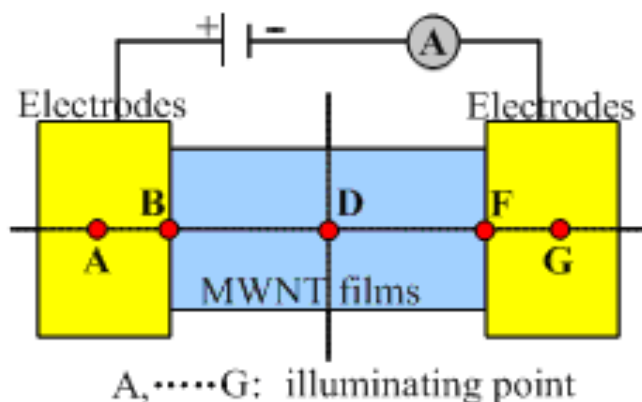


Fig. 3. Schematic illustration of MWCNT film/Al heterostructures.

point symmetry. As the laser-illuminating point moves from left electrode A to right electrode G, the photocurrent is almost 0 at position A, then decreases to the negative maximum at interface B, and becomes almost 0 at position D, which is approximately the geometric center of the film.

The generation of photocurrent involves photo absorption, electron–hole pair creation and charge transfer processes. Generally, CNTs are composed of metallic tubes and semiconducting tubes, and the junctions are formed between metallic and semiconducting CNTs. During laser illumination with photo energy larger than the semiconductor band gap, the photo-induced carriers generate in semiconducting CNTs. Meanwhile, the Schottky junctions are formed at the interface of MWCNTs and Al electrodes.

As shown in Fig. 5, if illumination point is position B, the electron–hole pairs are separated as electron and hole. Our sample is N semiconductor from Hall effect measurement, hence, next we will focus on

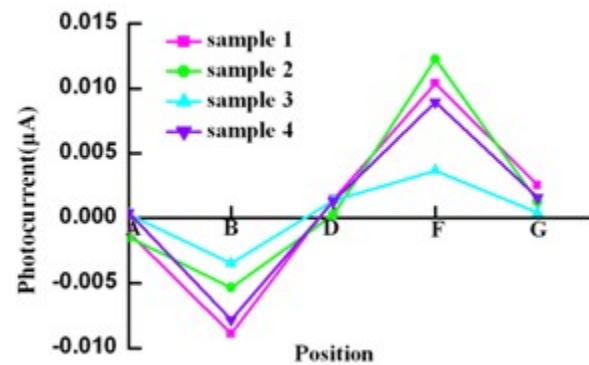


Fig. 4. Dependence of photocurrent at different illuminating positions.

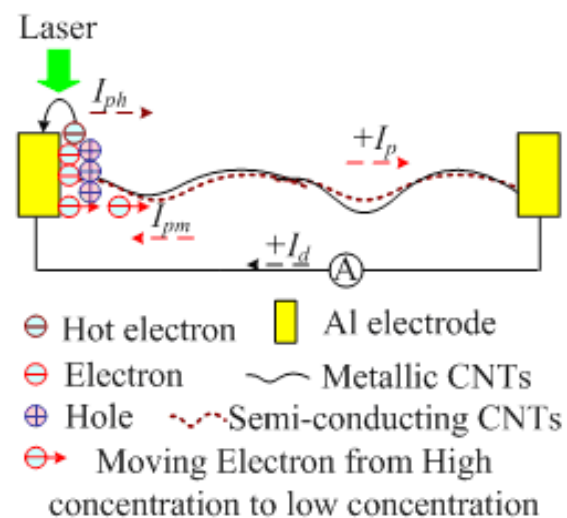


Fig. 5. Schematic representation of the operation of MWCNT sample. $+I_d$ is the positive direction of external current, $+I_p$ positive direction of photocurrent. The net photocurrent I_p is the sum of two reverse-direction currents I_{ph} and I_{pm} .

electron movement. Two processes are considered: (1) The hot electrons move swiftly across the Schottky barrier easily, and enter the positive metal Al electrode (Position B) before recombining with holes, which brings current I_{ph} , its direction is the reverse of the electron-moving direction. (2) More electrons are generated at position B (the electron's concentration at position B is higher than that at position F), where redundant electrons move from position B to position F. Thus, there is a current I_{pm} . So, the net photocurrent I_p is the sum of two reverse direction currents I_{ph} and I_{pm} . For our samples, we thought that most of the photo-induced electrons cannot go across the Schottky barrier, they congregate at position B and have high electron concentration; the current I_{pm} is larger than I_{ph} . The I_{pm} direction is reverse to $+I_p$. So at position B, the net photocurrent is negative. At position F, the net photocurrent is positive with the same explanation.

At position D, the hot electrons have the same chance and the same free length to bring the two metal electrodes, and most of the electrodes and holes would recombine and contribute little to the photocurrent. The photocurrents at position D should be 0, but not really 0 in experiments. One reason is that it is not exact geometric center according to the experimental handling error. The other reason is the sample's uniformity, which leads to different internally-built voltages at two MWCNT film/Al interfaces.

Another interesting observation worth noticing is zero-bias photocurrent at position B and F, which is about 0.01 μA . The photocurrent measurements on pure Al electrodes (at positions A and G) show almost no obvious response with and without laser illumination, which indicates that the electrodes are not responsible for the observed significant photocurrents. As shown in Fig. 4, the photocurrent at Position F is a little higher than that at Position B, which could be due to the opto-thermal effect, because the measurement point is from Position A to Position G, and the temperature increases as the illumination time increases. At higher temperature, more number of photon-generated electrons become 'hot' electrons with higher kinetic energy, resulting in a higher photocurrent^[7,23-26]. Sample's uniformity problem is another reason.

We fixed the laser spot position at the geometric center of the MWCNT films in order to avoid generation of the photo-induced voltage^[20]. The I - V characteristics of MWCNT films at room temperature are shown in Fig. 6. The net photocurrent I_p increases with increasing bias voltage, and is an almost linear function of the bias voltage. Once laser illumination is on, the current would increase dramatically to about 12.5 mA with a bias voltage of 2 V.

As shown in Fig. 7, due to the non-zero bias voltage applied, the separated electrons and holes orderly move to the corresponding electrodes effectively with the help of external electric field formed by the bias

voltage, and the flow of charge carriers contributes to the photocurrent.

The photocurrent induced by the laser can be described as^[27]

$$I_p = \eta q P_\lambda \mu \tau \lambda V_{bias} / h c l^2, \quad (1)$$

where, η is quantum efficiency, q is unit charge, G is the inner gain of sample, which is equal to τ / T_r , τ is free carrier lifetime, T_r is transit time of majority carrier, and $T_r = l^2 / \mu V_{bias}$, where l is channel length (electrode separation), μ is the mobility of majority of the carriers. N_λ is the number of photons of the wavelength absorbed in unit time, so $N_\lambda = P_\lambda / h c$, where P_λ is the monochromatic power. V_{bias} determines the transit time of the carrier, higher the V_{bias} , shorter the transit time, leading to higher photo-induced currents.

To access the sensitivity of the MWCNT films, a parameter is considered, i.e., its responsivity $Rv = \Delta I / \Delta P$. Here, ΔI is the net photocurrent; ΔP is the radiation power incident to the sample. In our experiments, $Rv = 0.4 \mu\text{A/W}$ at $V_{bias} = 0 \text{ V}$ and $Rv = 521 \text{ mA/W}$ at $V_{bias} = 2 \text{ V}$. In a study conducted by St-Antoine *et al.*^[16], for metal-MWCNT-metal heterodimension junctions illuminated by a 780-nm laser with 50 mW, the photocurrent was found to be about 5.8 μA . So, $Rv = 0.116 \text{ mA/W}$. In a study conducted by Sun *et al.*^[18], for a macrolong pure metal Ag nanowire bundle, the photocurrent was 25.5 μA and 98.9 μA at temperatures 304 K and 77 K, respectively, with a 142.3 mW laser illumination and a

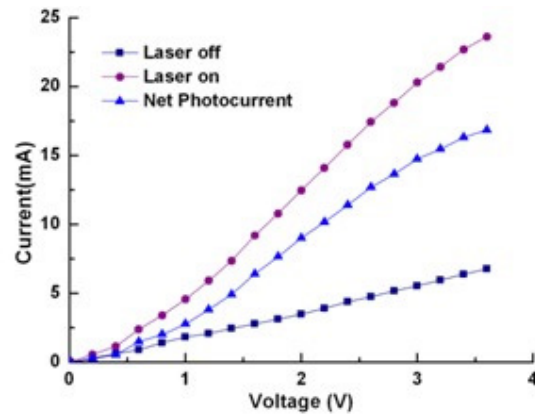


Fig. 6. Experimental current-voltage characteristics of MWCNT films.

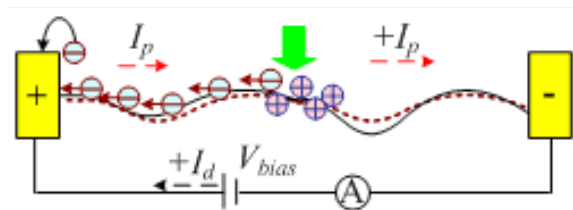


Fig. 7. Schematic diagram of generation and movement of photo-induced excitons, where I_p is photocurrent and I_p is positive because it is the same in the $+I_p$ direction.

bias voltage of 0.1 V. So, $Rv = 0.695$ mA/W at $T = 77$ K. For MWCNT–CuS hybrid^[19], the photocurrent was 20 nA with 550 nm laser with a power of 25 mW illumination at $V_{bias} = 0$ V, so, $Rv = 0.8$ μ A/W. Our samples including structure design, electrode chosen, and manufacturing step optimized should be improved in order to gain high responsivity.

Further studies need to be conducted for precision analysis of this position effect. First, perfecting the sample fabrications is an important step, including improving the uniformity of the MWCNT films, because the density of the CNTs under laser illumination determines the generation ratio of photo-excited carriers. Second, enhancing the symmetry of the Al electrodes, which affects the symmetry of the photocurrent–position curve. Third, the precision of moving distance should be controlled accurately. More data should be recorded by minimizing the moving step. Optimizing the design samples is another important and necessary improvement that needs to be done.

In conclusion, we demonstrate that the MWCNT films are capable of absorbing the laser and generating a photocurrent. The photocurrent of MWCNT sample exhibits a position effect, which is employed to develop a position photodetector. Further studies are required to develop and optimize the MWCNTs for precision measurement, photodetector and solar cell applications.

We would like to thank Prof. Xiaoxing Zhang, College of Electric Engineering, Chongqing University, for providing CNT materials. The work was funded by National Science Fund (No. 61376121), NSF of Chongqing Municipal, China (CSTC 2011BB2076), and the Fundamental Research Funds for the Central Universities (106112013CDJZR125502, 106112013CDJZR120003 and 106112013CDJZR120008) and Visiting Scholar Fund.

References

1. P. Chen, X. Wu, X. Sun, J. Lin, W. Ji, and K. L. Tan, *Phys. Rev. Lett.* **82**, 2548 (1999).
2. X. C. Liu, J. H. Si, B. H. Chang, G. Xu, Q. G. Yang, Z. W. Pan, S. S. Xie, and P. X. Ye, *Appl. Phys. Lett.* **74**, 164 (1999).
3. J. S. Lauret, C. Voisin, G. Cassabois, J. Tignon, C. Delalande, R. Ph, O. Jost, and L. Capes, *Appl. Phys. Lett.* **85**, 3572 (2004).
4. M. J. O'Connell, S. M. Bachilo, C. B. Huffman, V. C. Moore, M. S. Strano, E. H. Haroz, K. L. Rialon, P. J. Boul, W. H. Noon, C. Kittrell, J. Ma, R. H. Hauge, R. B. Weisman, and R. E. Smalley, *Science* **297**, 593 (2002).
5. R. J. Chen, N. R. Franklin, J. Kong, J. Cao, T. W. Tomblor, Y. G. Zhang, and H. J. Dai, *Appl. Phys. Lett.* **79**, 2258 (2001).
6. M. Freitag, Y. Martin, J. A. Misewich, R. Martel, and P. Avouris, *Nano Lett.* **3**, 1067 (2003).
7. I. A. Levitsky and W. B. Euler, *Appl. Phys. Lett.* **83**, 1857 (2003).
8. J. Wei, J. Sun, J. Zhu, K. Wang, Z. Wang, J. Luo, D. Wu, and A. Cao, *Small* **2**, 988 (2006).
9. P. Castrucci, F. Tombolini, M. Scarselli, E. Speiser, S. Del Gobbo, W. Richter, M. De Crescenzi, M. Diociaiuti, E. Gatto, and M. Venanzi, *Appl. Phys. Lett.* **89**, 253107 (2006).
10. U. Coscia, G. Ambrosone, A. Ambrosio, M. Ambrosio, F. Busolotti, V. Carillo, V. Grossi, P. Maddalena, M. Passacantando, E. Perillo, A. Raulo, and S. Santucci, *Solid State Sci.* **11**, 1806 (2009).
11. M. Passacantando, F. Busolotti, V. Grossi, S. Santucci, A. Ambrosio, and A. Raulo, *Appl. Phys. Lett.* **93**, 051911 (2008).
12. W. Feng, Y. Feng, Z. Wu, Z. Wu, A. Fujii, M. Ozaki, and K. Yoshino, *J. Phys. Condens. Mater.* **17**, 4361 (2005).
13. J. Zhang, Y. Q. Jiang, P. B. Wang, and H. L. Tian, *Microsyst. Technol.* **16**, 2115 (2010).
14. P. Stokes, L. W. Liu, J. H. Zou, L. Zhai, Q. Huo, and S. I. Khondaker, *Appl. Phys. Lett.* **94**, 042110 (2009).
15. M. S. Fuhrer, J. Nugard, L. Shih, M. Forero, Y. G. Yoon, M. S. Mazoni, H. J. Choi, I. Ihm, S. G. Louie, A. Zettl, and P. L. McEuen, *Science* **288**, 494 (2000).
16. B. C. St-Antoine, D. Ménard, and R. Martel, *Nano Lett.* **11**, 609 (2011).
17. J. L. Sun, J. Wei, J. L. Zhu, D. Xu, X. Liu, H. Sun, D. H. Wu, and N. L. Wu, *Appl. Phys. Lett.* **88**, 131107 (2006).
18. J. L. Sun, J. Xu, J. L. Zhu, and B. L. Li, *Appl. Phys. A* **91**, 229 (2008).
19. Z. Y. Zhan, C. Liu, L. X. Zheng, G. Z. Sun, B. S. Li, and Q. Zhang, *Phys. Chem. Chem. Phys.* **13**, 20471 (2011).
20. R. A. DiLeo, B. J. Landi, and R. P. Raffaele, *J. Appl. Phys.* **101**, 064307 (2007).
21. J. Schwan, S. Ulrich, V. Batori, H. Ehrhardt, and S. R. P. Silva, *J. Appl. Phys.* **80**, 440 (1996).
22. J. L. Sun, W. Zhang, J. L. Zhuand, and B. Yang, *Opt. Express.* **18**, 4066 (2010).
23. A. Serra, D. Manno, E. Filippo, A. Tepore, M. L. Terranova, S. Orlanducci, and M. Rossi, *Nano Lett.* **8**, 968 (2008).
24. Y. Wang, K. Kempa, B. Kimball, J. B. Carlson, G. Benham, W. Z. Li, T. Kempa, J. Rybczynski, A. Herczynski, and Z. F. Ren, *Appl. Phys. Lett.* **85**, 2607 (2004).
25. S. X. Lu and B. Panchapakesan, *Nanotechnology* **17**, 1843 (2006).
26. P. M. Ajayan, M. Terrones, A. de la Guardia, V. Huc, N. Grobert, B. Q. Wei, H. Lezec, G. Ramanath, and T. W. Ebbesen, *Science* **296**, 705 (2002).
27. Y. J. Pan and J. Zou, *Photoelectronic Technique* (in Chinese) (Chongqing University Press, Chongqing, 2000).